

**CFA** **8:00 am–9:45 am**  
Room 318/320

**Dispersion Managed Solitons**

Walter I. Kaechele, CODEON Corp., USA, President

**CFA1 (Tutorial) 8:00 am**

**Linear and nonlinear effects in lightwave transmission: Dispersion management in terrestrial and submarine systems**

Jean-Pierre Hamaide, Alcatel, France

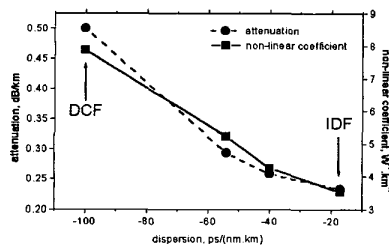
Summary not available.

**CFA2 9:00 am**

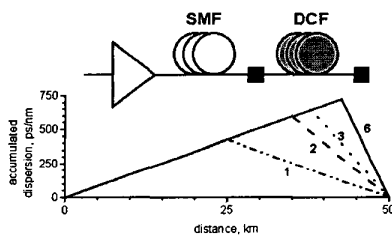
**System Performance of New Types of Dispersion Compensating Fibres**

C. Peucheret,<sup>1</sup> T. Tokle,<sup>1</sup> S.N. Knudsen,<sup>1,2</sup> C.J. Rasmussen<sup>1</sup> and P. Jeppesen,<sup>1</sup> <sup>1</sup> Research Center COM, Technical University of Denmark, 2800 Lyngby, Denmark; Email: cp@com.dtu.dk; <sup>2</sup> Lucent Technologies Denmark, Priorparken 680, 2605 Brøndby, Denmark Email: sknudsen@lucent.com

The management of dispersion and non-linearities is of prime importance in WDM systems. Dispersion compensating fibres (DCF) are extremely attractive when used in conjunction with standard single mode fibres (SMF). New types of DCFs compensating for the dispersion of SMF in a 1:1 length ratio have been recently presented<sup>1,2</sup> and intermediate types of DCF (compensating for SMF in a 1:2 or 1:3 length ratio) have also been designed and fabricated in the present work. The properties of the various types of available DCFs



CFA2 Fig. 1. Evolution of the dispersion compensating fibres attenuation and non-linear coefficient as a function of dispersion (based on average measurements on manufactured fibres).

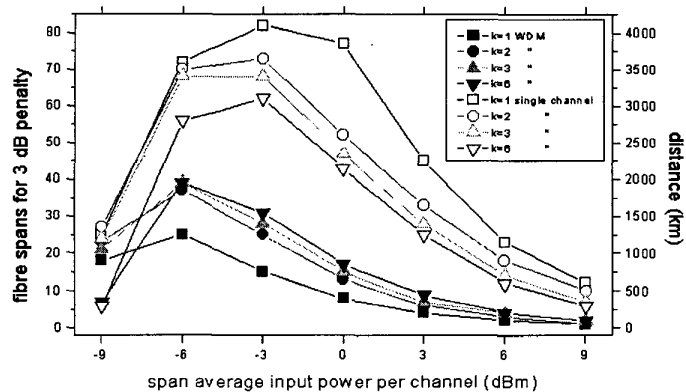


CFA2 Fig. 2. Dispersion maps under investigation for SMF to DCF length ratios between 1 and 6.

with dispersion of -17, -40, -54 and -100 ps/(nm.km), corresponding to SMF to DCF length ratios of about k = 1 (inverse dispersion fibre - IDF), 2, 3 and 6 (conventional DCF) respectively are shown in Fig. 1. All these fibres also provide dispersion slope compensation. It can be seen that when the absolute value of the dispersion is reduced from DCF to IDF values, both attenuation and non-linear coefficient are significantly reduced. As all these new fibres are designed to be cabled (therefore the DCF is part of the span length), and as it has also been shown that conventional DCF can be cabled successfully,<sup>3</sup> their use in real systems needs to be compared.

In spans like the ones in Fig. 2, and assuming a constant span length, the DCF will be placed closer to optical amplifiers when the absolute value of its dispersion is reduced from conventional DCF to IDF values. Therefore a trade-off has to be found between increased input power and decreased non-linear coefficient, resulting in an optimal dispersion map. Numerical simulations based on the split-step method have been performed to compare the different dispersion maps in Fig. 2 for a fixed span length of 50 km and for NRZ modulation at 10 Gbit/s. The interaction of dispersion, Kerr-effect non-linearities and amplifier noise is included in the simulations. WDM simulations have been performed on an 8 channel system with 35 GHz spacing in order to investigate the effects of cross-channel non-linear effects. Pseudo random sequence lengths of 1024 bits were used in the simulations for realistic penalty calculations, and WDM channels were uncorrelated.

Fig. 3 shows the maximum number of spans which can be cascaded for 3 dB power penalty (PIN receiver) as a function of SMF average input power per channel. For WDM transmission, only the worst-case channel is represented (one of the innermost channels). In the single channel case, k = 1 performs the best whatever the power level and proves to be more robust to self-phase modulation. Owing to increased span loss, k = 6 shows degraded performance at low power levels where the system is limited by noise. The poorer performance seen in the WDM case is attributed to cross-phase modulation which reduces the efficiency of the k = 1 span when the system is no longer noise limited. Therefore k = 2 and 3 appear as good compromises for WDM, offering lower span loss than conventional DCF while still being resistant to cross-phase modulation.



CFA2 Fig. 3. Number of cascaded spans for 3 dB penalty as a function of span average input power per channel for single and 8 channel WDM transmission (worst channel)

**References**

1. K. Mukasa, Y. Akasaka, Y. Suzuki, and T. Kamiya, "Novel network fiber to manage dispersion at 1.55  $\mu\text{m}$  with combination of a 1.3  $\mu\text{m}$  zero dispersion single mode fiber," in *Proc. ECOC'97*, Edinburgh, Scotland, pp. 127–130.
2. S.N. Knudsen, and T. Veng, "Large effective area dispersion compensating fiber for cabled compensation of standard single mode fiber," in *Proc. OFC'2000*, Baltimore, Maryland, paper TuG5.
3. L. Grüner-Nielsen, S.N. Knudsen, B. Edvold, T. Veng, D. Magnussen, C.C. Larsen, and H. Damsgaard, "Dispersion compensating fibers," *Opt. Fiber Technol.* 6, 164–180 (2000).

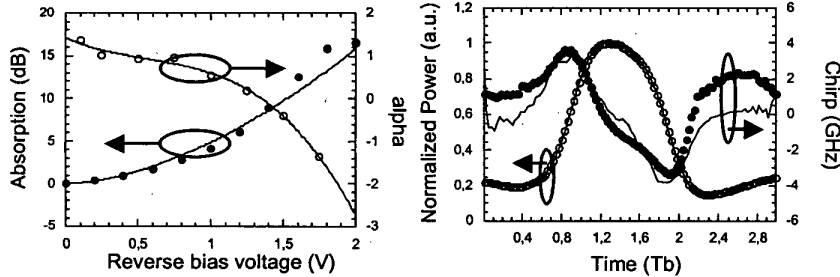
**CFA3 9:15 am**

**10 Gb/s uncompensated transmission in transparent optical metropolitan area networks using electroabsorption modulators over negative dispersion fiber**

I. Roudas, N.M. Lascar(+), A.E. Kruse, B.S. Hallock, D.Q. Chowdhury(+), R.S. Vodhanel, N. Antoniadis, I. Tomkos, and M. Sharma, *Photonic Research and Test Center, Corning Incorporated, 2200 Cottontail Lane., Somerset, New Jersey 08873; Email: roudasj@corning.com (+) Communications Department., ENST Paris, 46 r. Barrault, 75634 Paris Cedex 13, France; (\*) Science and Technology Division, Corning Incorporated, Corning, New York, 14831*

Integrated electroabsorption modulator-DFB lasers (EA-DFBs) are attractive candidates for 10 Gb/s transmission due to their low cost, compact size, high output power, and good extinction ratio. This paper presents, for the first time, a theoretical and experimental study of the performance of EA-DFBs for WDM 10 Gb/s NRZ transmission in transparent optical metropolitan area networks (MANs)<sup>1</sup> using negative dispersion fiber.

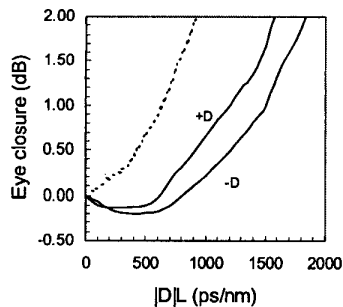
In the simulation, a phenomenological model of the EA-DFBs based on measurements of the absorption and the alpha parameter as a function of the applied reverse bias voltage is used.<sup>2</sup> Fig. 1(a) shows the absorption and the alpha parameter characteristics for a commercially-available EA-DFB operating at 1548.7 nm, measured using the method described in.<sup>3</sup> For the same device,



**CFA3 Fig. 1.** (a) Absorption and small-signal alpha parameter of a commercially-available integrated EA-DFB (Points = measurements, lines = fitting); (b) Power and time-resolved chirp waveforms (Points = measurements, lines = model,  $T_b$  = bit period).

Fig. 1(b) compares measured and theoretical power and time-resolved chirp waveforms for an isolated one surrounded by zeros and shows that they are in good agreement.

Using the aforementioned EA-DFB model and the measurements of Fig. 1, we first studied the transmission of 10 Gb/s NRZ signals over positive and negative dispersion fibers in the absence of fiber nonlinear effects. Fig. 2 shows the dispersion induced eye-closure penalty versus  $|D|L$  product for both fiber types (solid lines). In each case, the bias and modulating voltage of the absorption section of the EA-DFB are optimized in order to achieve maximum transmission distance. For comparison, the dispersion induced eye-closure penalty for an ideal ASK waveform with zero chirp and infinite extinction ratio is shown (broken line). For this particular device, it is observed that there is no significant difference in the dispersion budget for fibers with the same absolute value, but opposite signs, of the dispersion parameter. This observation is verified experimentally for three additional commercially-available devices which exhibit dispersion budgets of 1325–1701 ps/nm over negative dispersion fiber vs. 1333–1684 ps/nm over positive dispersion fiber for  $Q \geq 8.5$  dB (corresponding to a bit error rate less than  $10^{-12}$ ). It should be stressed however that in all cases, higher output powers (typically by 8 dB) are achieved for negative dispersion fibers. In addition, for certain EA-DFBs which exhibit only positive alpha parameter values,<sup>2</sup> the use of negative dispersion fiber is

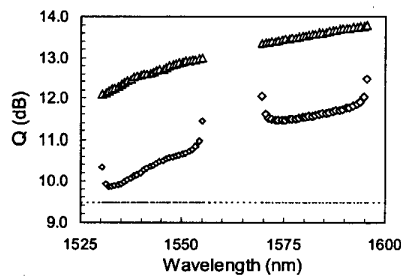


**CFA3 Fig. 2.** Dispersion induced eye closure penalty versus  $|D|L$  product (Conditions: solid lines = DFB-EA waveforms, broken line = ideal ASK waveform with zero chirp and infinite extinction ratio. Timing jitter of 12 ps at the sampling instant is assumed.)

clearly beneficial. In conclusion, negative dispersion fibers allow simultaneous optimization of the power and dispersion budgets of EA-DFBs.

In order to investigate the impact of nonlinear effects, we performed a simulation study of a chain of six equidistant Wavelength Add-Drop Multiplexers (WADMs) separated by five spans of MetroCor<sup>TM</sup> fiber. The latter exhibits a dispersion parameter of about  $-3$  ps/nm/km in the L-band and above  $-8$  ps/nm/km in the C-band<sup>4</sup> and has an effective area comparable to other non-zero dispersion-shifted fibers (NZDSFs). A reasonable worst case scenario is assumed: The network length is 200 km; Each WADM is represented as an amplifier with flat gain equal to the span loss and an effective noise figure equal to 8 dB;<sup>5</sup> The optical power launched into the fiber is 0 dBm/channel; The channel spacing is 100 GHz.

Fig. 3 shows the theoretical Q-factor as a function of the channel wavelength for 32 10 Gb/s NRZ channels in the C- and L-band respectively. In the absence of fiber nonlinearities (triangles), it is observed that Q varies  $\sim 1$  dB between the edge channels of each band and increases monotonically from short to long wavelengths following the corresponding variation of the dispersion parameter. With fiber nonlinearities included (diamonds), the Q-factor for all channels decreases due to the small effective area but is still above 9.5 dB (horizontal line) (error probability less than  $10^{-15}$ ) at the beginning of the life of the network. This provides a 1 dB margin above the target Q-factor of 8.5 dB at the end of life of the life of the network. A detailed com-



**CFA3 Fig. 3.** Theoretical Q-factor as a function of the channel wavelength after 5 spans of 40 km MetroCor fiber (Conditions: triangles = no fiber nonlinearities, diamonds = with fiber nonlinearities).

parison for different power levels, fiber types, and modulation formats will be reported at the conference.

#### References

1. A.M. Saleh and J.M. Simmons, *J. Lightwave Technol.*, vol. 17, No. 12, pp. 2431–2448, 1999.
2. J.C. Cartledge and B. Christensen, *J. Lightwave Technol.*, vol. 16, No. 3, pp. 349–357, 1998.
3. F. Devaux et al, *J. Lightwave Technol.*, vol. 11, No. 12, pp. 1937–1940, 1993.
4. M. Sharma et al., *NFOEC*, Vol. 1, pp. 27–34, Denver, CO., 2000.
5. N. Antoniadis et al., *LEOS summer topical meeting*, Orlando, FL, 2000.

#### CFA4

9:30 am

#### Spectral efficiency of dispersion managed solitons: comparison of 20, 40 and 80 Gbit/s based WDM transmission

L.J. Richardson, V.K. Mezentsev and S.K. Turitsyn, *Photonics Research Group, Aston University, Birmingham, B4 7ET, UK; Email: richarlj@aston.ac.uk*

The current methodology of high capacity systems design focuses around the use of many wavelength channels each operating at a relatively low bit rate.<sup>1–3</sup> However, with the advancements in single channel performance brought by short period dispersion management,<sup>4</sup> it is now feasible to consider the possibility of WDM systems using fewer wavelength channels operating at higher bit rates. Reduction of the number of channels appears attractive for the design of cost effective systems but one must also consider the impact on system performance. With this intention, we investigate the performance of three specific systems using  $16 \times 20$  Gbit/s,  $8 \times 40$  Gbit/s and  $4 \times 80$  Gbit/s WDM transmission.

For an amplifier span  $Z_a = 40$  km, we fix the dispersion map strength  $S \approx 2$  by adjusting the dispersion management period ( $Z_d$ ) for each of the pulse widths. This ensures that for each pulse width we have the propagation characteristics of the conventional dispersion managed soliton. To provide a more fair comparison we fix the ratio of bit rate ( $\tau_{bit}$ ) to pulse-width ( $\tau$ ) to channel spacing ( $\Delta C$ ) giving the following parameters: for 20 Gbit/s  $\tau = 20$  ps,  $\Delta C = 75$  GHz; for 40 Gbit/s  $\tau = 10$  ps,  $\Delta C = 150$  GHz, and for 80 Gbit/s  $\tau = 5$  ps,  $\Delta C = 300$  GHz. The dispersion maps are constructed using SMF and RDF sections and a residual dispersion slope of 0.01 ps/nm<sup>2</sup>/km is introduced.

Figures 1–3 illustrate the single channel and WDM performances of the  $16 \times 20$  Gbit/s,  $8 \times 40$  Gbit/s and  $4 \times 80$  Gbit/s transmission using pre-chirped Gaussian pulses. It is apparent from figures 1–3 that for both single channel and WDM transmission the 20 Gbit/s systems display the best performance. The inherent manifestations of scaling bit rates<sup>5</sup> are visible for the 40 Gbit/s and 80 Gbit/s based transmission where for the single channel case, the dependencies gain a certain sharpness in their characteristics, which is indicative of the increasing sensitivity to initial conditions. Common to all of the systems is the large WDM penalty due to inter-channel interactions; however, as the bit rate per wavelength increases